Cessation of deep convection in the open Southern Ocean under anthropogenic climate change

Casimir de Lavergne[1]*, Jaime B. Palter[1], Eric D. Galbraith[2], Raffaele Bernardello[3] and Irina Marinov[3]

In 1974, newly available satellite observations unveiled the presence of a giant ice-free area, or polynya, within the Antarctic ice pack of the Weddell Sea, which persisted during the two following winters[1]. Subsequent research showed that deep convective overturning had opened a conduit between the surface and the abyssal ocean, and had maintained the polynya through the massive release of heat from the deep sea[2,3]. Although the polynya has aroused continued interest[1-9], the presence of a fresh surface layer has prevented the recurrence of deep convection there since 1976[8], and it is now largely viewed as a naturally rare event[10]. Here, we present a new analysis of historical observations and model simulations that suggest deep convection in the Weddell Sea was more active in the past, and has been weakened by anthropogenic forcing. The observations show that surface freshening of the southern polar ocean since the 1950s has considerably enhanced the salinity stratification. Meanwhile, among the present generation of global climate models, deep convection is common in the Southern Ocean under pre-industrial conditions, but weakens and ceases under a climate change scenario owing to surface freshening. A decline of open-ocean convection would reduce the production rate of Antarctic Bottom Waters, with important implications for ocean heat and carbon storage, and may have played a role in recent Antarctic climate change.

Antarctic Bottom Water (AABW) is the coldest, densest and most voluminous[11] water mass of the world ocean and its shrinking in recent decades[12,13] has been linked to deep ocean heat uptake[12,14]. Produced at present on Antarctic continental shelves, AABW is exported northwards to fill the deepest layers of the three oceanic basins and feed the deep branch of the meridional overturning circulation[11,15]. In 1928, on the basis of early hydrographic observations, it was suggested[16] that open-ocean convection also contributes to the production of AABW, as it does to North Atlantic Deep Water in the Labrador Sea. It was argued that deep convection occurred within the Weddell Gyre, but because of difficulty monitoring the Weddell Sea during austral winter, this contention went unverified until the mid-1970s[6].

Microwave observing satellites were first launched in December 1972, providing global observations of sea ice, and soon thereafter revealed the presence of a 250,000-km² ice-free area within the seasonally ice-covered Weddell Sea[1] (Fig. 1a). The huge polynya, located near Maud Rise (65° S, 0°), reappeared during the winters of 1974 to 1976, slowly drifting westward with the background

flow[1]. The polynya was maintained by vigorous convective mixing, whereby the upward flux of relatively warm deep waters supplied enough heat to prevent sea ice formation[1-3]. Heat loss at the surface drove cooling to depths of about 3,000 m, producing new deep waters[3] that could have fed the observed surge in Southern Ocean AABW volume during the following decade[13]. Together with the inference from hydrographic data of a Weddell convective event circa 1960[3], these observations confirm that deep convection in the open Weddell Sea has been a significant mode of AABW ventilation[5,6]. However, following 1976, no similar polynya has been observed. The continuing quiescence over the past 37 of 41 available years of satellite observation makes it tempting to assume that deep convection in the open Southern Ocean occurs rarely, with little global consequence. Here we propose, instead, that deep convection was more common in the pre-industrial state, but that the hydrological changes associated with global warming[17-19] are now suppressing this convective activity.

The high-latitude Southern Ocean is weakly stratified, with a cold, fresh surface layer overlying a warmer, saltier interior of nearly identical density[6,20]. Weddell Sea convection is thought to occur when the weak stratification is overcome by low-frequency variability in precipitative–evaporative fluxes[8,21], brine rejection during sea ice formation[2], or circulation–topography interactions[7,20]. Wind variability may participate in polynya initiation through spin-up of the cyclonic gyre, enhancing Ekman upwelling at the gyre centre and uplift at Maud Rise[20], or by dynamically[9] and thermodynamically[4] weakening the ice pack. Thermobaric effects, which cause the cold surface waters to become relatively denser as they sink, abruptly extend the depth of convective overturning once it begins[22]. Deep convective mixing may continue until an excessive surface freshwater supply[2,23] or the exhaustion of the deep heat reservoir[23] allows column re-stratification.

It has been suggested that a persistent positive phase in the Southern Annular Mode, brought on by stratospheric ozone depletion and rising CO₂ concentrations, may be delaying the return of the Weddell Polynya by inhibiting the re-establishment of the dry atmospheric conditions and associated high surface salinities favourable for destabilizing the winter halocline[8]. However, given that increasing inputs of fresh water to the southern high-latitude ocean over the past 50 years are well documented[17-19], a long-term, large-scale upper-ocean stratification trend could be expected to be superimposed on interannual and decadal variability. To evaluate

¹Department of Atmospheric and Oceanic Sciences, Burnside Hall, McGill University, 805 Sherbrooke Street West, Montreal, Quebec H3A 0B9, Canada, ²Department of Earth and Planetary Sciences, McGill University, 3450 University Street, Montreal, Quebec H3A 0E8, Canada, ³Department of Earth and Environmental Science, Hayden Hall, University of Pennsylvania, 240 S. 33rd Street, Philadelphia, Pennsylvania 19104-6316, USA.
*e-mail: casimir.delavergne@gmail.com
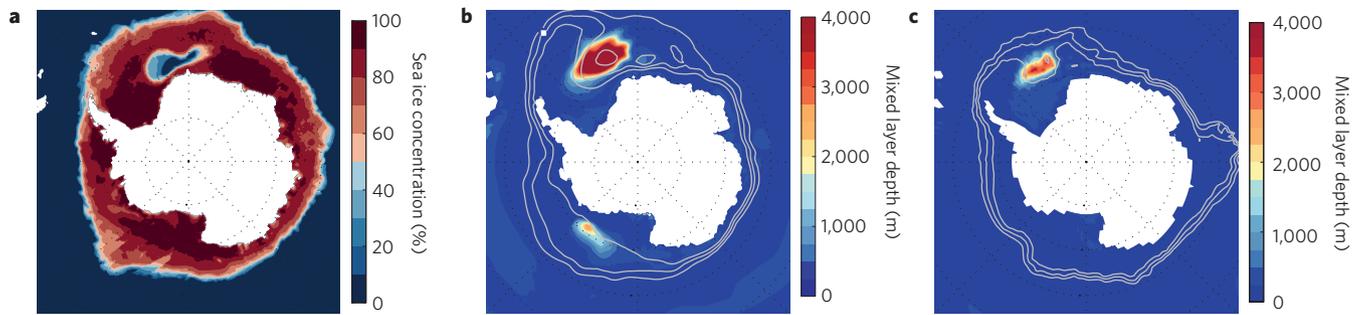
Figure 1 | Spatial pattern of Southern Ocean deep convection in observations and models. a, Observed 1974–1976 mean September sea ice concentration (%) from Nimbus-5 ESMR Polar Gridded Sea Ice Concentrations[30] delineating the Weddell Polynya extent. **b**, September mixed layer depth (shading) and 25%, 50% and 75% September sea ice concentration contours (grey lines) in the MPI-ESM-LR model, averaged over pre-industrial control years during which the convection area exceeds half of its overall maximum. **c**, The same as in **b**, but for the HadGEM2-ES model. Deep mixed layers, coinciding with anomalously low sea ice concentrations, are found over an area of comparable size to the Weddell Polynya and in a similar location. The spatial pattern of deep convection in all convective models is presented in Supplementary Fig. 1.
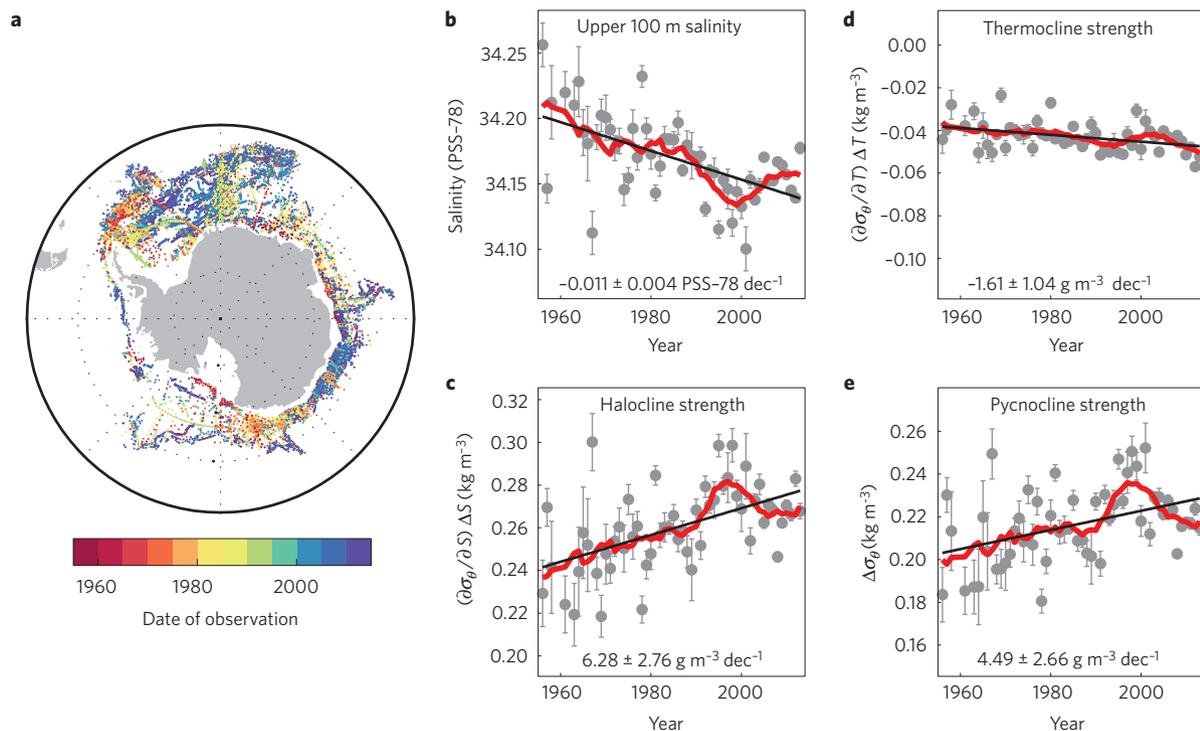
Figure 2 | Southern polar ocean freshening and stratification. a, Spatial distribution (dots) and year of observation (colour) of the 20,613 profiles included in this study. Excluding years with observations in fewer than 20 half-degree grid squares results in quasi-continuous coverage from 1956 onwards (Methods). Data from the BLUELink Ocean Archive[28]. **b–e**, Annual mean (± one standard error, grey), 10-year running mean (red) and linear trend (black) of 0–100 m salinity (**b**), halocline strength (**c**), thermocline strength (**d**) and pycnocline strength (**e**). The density stratification (**e**; $\Delta\sigma_\theta$) and its salinity (**c**; $(\partial\sigma_\theta/\partial S)\Delta S$) and temperature (**d**; $(\partial\sigma_\theta/\partial T)\Delta T$) components are calculated as differences between 100–200 m and 0–100 m, and presented with equal vertical range for comparison. Decadal trends with their 95% confidence intervals are indicated at the bottom.

this possibility, we examined 20,000 profiles of salinity and temperature selected to lie within the southern polar ocean, south of the Antarctic Circumpolar Current, but excluding the Antarctic continental shelf (Methods; Fig. 2a). Despite the historically sparse data coverage, significant circumpolar, area-averaged surface freshening over the past 60 years is detected (Fig. 2b). As the surface layer has become more buoyant, both vertical salinity and temperature gradients have intensified (Fig. 2c,d). As a result of the strong salinity control on density at the prevailing near-freezing temperatures, the salinity contribution to the density stratification dominates, resulting in increased stability (Fig. 2e). This long-term freshening of southern polar surface waters is consistent

with changes in the precipitation–evaporation balance related to global water cycle amplification[17] and the positive Southern Annular Mode trend[8,18], and with accelerating melting and calving of Antarctic glaciers[19].

To explore the potential sensitivity of open-ocean deep convection to Southern Ocean freshening under anthropogenic climate change, we examined 36 models of the most recent Coupled Model Intercomparison Project (CMIP5; ref. 24). Although these models lack fully interactive land ice and cannot simulate increased glacial melt in response to ocean warming (Supplementary Information), they simulate changes in precipitation, evaporation, winds, sea ice and ocean circulation. Twenty-five models were found

to exhibit significant deep (>2,000 m) open-ocean convection between 90° S and 55° S under pre-industrial conditions (Methods). We stress here the caveat that these global climate models are too coarse to capture the export of dense shelf waters along the continental slope, and therefore miss this important source of deep ocean ventilation[10]. The lack of downslope currents could cause the Southern Ocean to be too weakly stratified, making it more prone to convective activity. Consequently, the simulated convection may be unrealistically strong in some cases, with reduced sensitivity to freshwater loading. On the other hand, the fact that convective chimneys have been clearly observed in the Weddell Sea[3,5,6] implies that the non-convecting models are missing a real mode of Southern Ocean ventilation. Indeed, models with no convective activity more often have overly strong vertical stratification, excessive summer ice coverage, or both[10] (Supplementary Fig. 3).

The areal extent of convection averages 930,000 km² over pre-industrial control years across the 25 convecting models. The Weddell and Ross gyres generally host most of the deep convection, but some models also place convective chimneys in the Indian and eastern Pacific sectors (Supplementary Fig. 1). Figure 1b,c shows the spatial pattern of convection simulated by two models, chosen for their accurate simulations of AABW properties[10] and extended climate change experiments (continuing to 2300), that provide among the best qualitative representations of the Weddell Polynya in size, location and intensity of the deep convection. The frequency of convective events is variable across models (Supplementary Table 1 and Fig. 2), reflecting the sensitivity of convection to features of ocean circulation, air–sea fluxes, sea ice[23] and model resolution[25]. Eleven of the models simulate convection almost every winter, whereas multiple decades can separate convective events in some weakly convecting models. By averaging over the 25-model ensemble, we find that 63% of all model years exhibit deep convection in the Southern Ocean, with a mean spacing between convective events of 10 years.

When subjected to increasing CO_2 concentrations following historical and Representative Concentration Pathway 8.5 (RCP8.5) forcings (Methods), all convecting models show a decrease in the strength of deep convection over the course of years 1900 to 2100 (Fig. 3 and Supplementary Table 2), with seven models exhibiting a complete cessation before 2030 (Supplementary Table 1). Simulations continued to year 2300 show no return of deep convection over this period. The fact that the slowing of Southern Ocean ventilation is so common across models suggests that a shared process is hampering the development of deep convective chimneys under warming conditions.

To explore the mechanisms driving the shutdown of convection under RCP8.5, we performed additional climate change experiments with a model (CM2Mc) featuring strong, episodic Weddell Sea ventilation events[21]. In a three-member ensemble using this model (Supplementary Information), the final convection events ended in years 1952, 1987 and 2005, highlighting the intrinsic variability and sensitivity to initial conditions of the convection cycles. Enhanced freshwater input south of 45° S, driven by increased precipitation and decreased evaporation (Supplementary Fig. 4), contributes to strengthening the halocline, building an efficient barrier to convective mixing. To test the role of the surface freshwater balance versus that of wind stress changes on ocean circulation, we made two additional sets of simulations with CM2Mc: one three-member ensemble in which we applied only the precipitation–evaporation changes over 90° S–40° S and another in which only global wind stress changes were applied (Supplementary Fig. 5). With the application of the wind stress perturbation alone, convection shifted from the Weddell Sea to the Ross Sea, but there was no significant decrease in overall deep Southern Ocean ventilation (Supplementary Fig. 6). In contrast, the precipitation–evaporation perturbation south of 40° S alone was
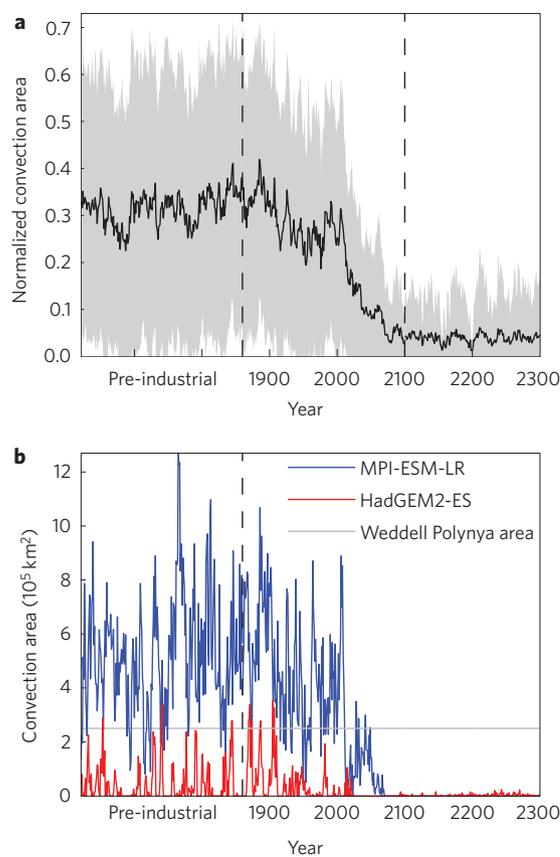
Figure 3 | Southern Ocean (55° S–90° S) convection area. a, Ensemble mean (black line) and multi-model standard deviation (grey shading) of normalized convection areas in the 25 CMIP5 convecting models. For each model, the area is normalized by the maximum areal extent of convection recorded in the entire simulation. Shown are the last 240 years of pre-industrial control runs followed by historical (1860–2005) and RCP8.5 (2006–2300) simulations. Only eight models were run beyond year 2100. **b**, Convection area in the MPI-ESM-LR (blue) and HadGEM2-ES (red) models. The 1974–1976 Weddell Polynya area[1] is indicated by the light grey line for comparison.

sufficient to stop the deep convection, with the latest convection events ending in years 1977, 1989 and 2021 for each ensemble member. We conclude that the decrease in ventilation of Southern Ocean deep and intermediate waters simulated under RCP8.5 can be explained by altered surface freshwater fluxes at southern high latitudes (Supplementary Fig. 6).

As in CM2Mc and the observational record (Fig. 2), surface freshening of the southern polar ocean is observed in 34 of the 36 CMIP5 models and significantly exceeds unforced multidecadal variability in all but two of these models (Fig. 4a and Supplementary Fig. 7). The resulting increase of salinity stratification causes the model pycnoclines to strengthen (Fig. 4b). On average, the stratification strengthens later and more slowly in convecting models than in non-convecting models, owing in part to the disruption of freshwater build-up at the surface by convective exchange with saltier deep waters. Therefore, any tendency of convective models to overestimate convection probably delays their response to a perturbed freshwater balance in comparison with the real ocean: models with more extensive convection areas generally convect further into the twenty-first century (Supplementary Fig. 8). In addition, as CMIP5 models do not include the additional freshwater input from increased glacial melt, they probably underestimate the rate of freshening under climate
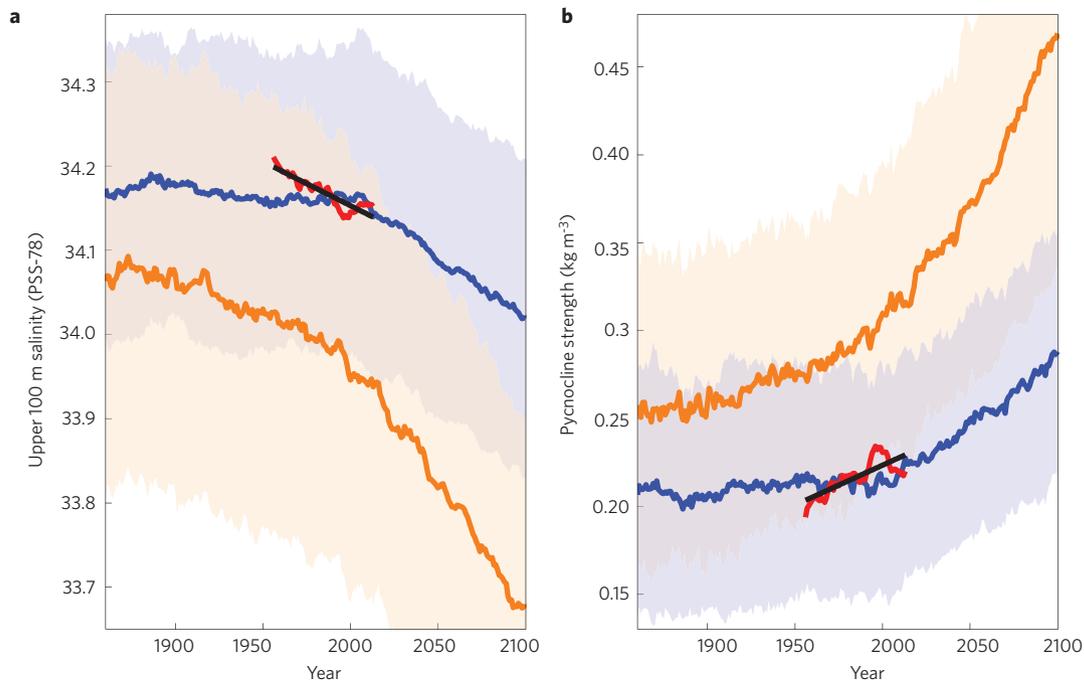
Figure 4 | Southern polar ocean freshening and stratification in CMIP5 models. a,b, Ensemble mean 0–100 m salinity (**a**) and pycnocline strength (**b**) of 25 convecting (blue) and 11 non-convecting (orange) CMIP5 models run over the twenty-first century with the RCP8.5 scenario. Both are annual means averaged over the area situated south of the Antarctic Circumpolar Current (where the surface dynamic height relative to 1500 m is less than its minimum within Drake Passage), excluding shelf waters. Shadings correspond to one multi-model standard deviation. The 10-year running mean (red) and linear trend (black) from the corresponding observations shown in Fig. 2 are repeated here for comparison.

warming. Indeed, freshening and stratification rates equivalent to those observed over 1956–2013 are not simulated by the ensemble of convecting models until the first half of the twenty-first century (Fig. 4), the period when the modelled convection strength undergoes its sharpest decrease (Fig. 3). In short, the CMIP5 model ensemble is consistent with a weakening of deep Southern Ocean convection under anthropogenic change, due to approximately the same degree of surface freshening and stratification as we find in the observational record.

The estimated 2–3 Sv of near-freezing surface waters that ventilated the upper AABW layer of the Weddell Sea during the three observed polynya years[3] represent a significant addition to the 5.4 ± 1.7 Sv of shelf water input to the bottom layer of the Southern Ocean[15]. Hence, a decreased frequency of deep convection would be expected to have slowed AABW production[3], and could have affected the denser shelf-produced AABW by altering the properties of deep waters involved in its formation and subsequent mixing[3,13]. The recent absence of Weddell Sea convection could thus be contributing to the observed widespread warming and volume loss of AABW[12,13].

A regime shift in Southern Ocean deep ventilation would also have had impacts on the air–sea exchange of heat and carbon. The heat release from the Weddell Polynya over 1974–1976 was estimated to be 0.4×10^{21} J yr^{-1} (ref. 3), nearly 10% of the average annual rise in ocean heat content over the 1972–2008 period[26]. Hence, stratification in the Weddell Sea may have increased ocean heat storage and attendant thermosteric sea level rise, and slowed warming of the atmosphere. Indeed, it has been suggested that decelerations of global warming are related to increased deep ocean heat storage, with a role for reduced AABW formation[14]. The recent absence of deep open-ocean convection could be contributing to contemporary trends in Southern Hemisphere climate, including slowed surface warming, subsurface ocean warming, sea ice expansion and poleward-

intensifying surface westerlies[25]. In addition, by exchanging with the vast deep ocean carbon pool, Weddell convective events would have modified atmospheric pCO$_2$. It is possible that Southern Ocean deep convection also varied significantly during past, natural climate changes, such as on centennial timescales of recent millennia[25] and during the last deglaciation, when proxies suggest marked ventilation changes in the deep South Atlantic[27]. Further proxy studies from the Weddell Sea may be able to shed light on these possibilities.

Methods

Observational record. All profiles were taken from the latest version of the BLUELink Ocean Archive[28]. We also used salinity and temperature monthly climatologies from the CSIRO (Commonwealth Scientific and Industrial Research Organisation) Atlas of Regional Seas[28] (CARS 2009), which is built from the same database. We first selected profiles with sufficient depth coverage for which the 0–1,500 m dynamic height is less than the CARS monthly minimum within Drake Passage (5.1–5.7 dyn dm). This dynamic height criterion allows a focus on profiles south of the Antarctic Circumpolar Current. To optimize the use of the relatively sparse data, an equivalent 0–500 m dynamic height threshold (2.2–2.6 dyn dm) was determined using the strong relationship between 0–1,500 m and 0–500 m dynamic heights, as obtained from a simple linear regression. This enabled us to include additional profiles covering only the 0–500 m depth range.

Salinity, *in situ* temperature and surface-referenced potential density were averaged over 0–100 m and 100–200 m for every profile. The derivatives of potential density with respect to salinity and temperature are also calculated and averaged over 0–200 m to obtain the individual contributions of salinity and temperature to the vertical density gradient. To avoid the aliasing of spatial and seasonal variability, we subtract the appropriate monthly gridded (0.5° × 0.5°) CARS atlas values from the 0–100 m and 100–200 m profile means. Yearly anomalies are then constructed as area-weighted averages over the sampled monthly, 0.5° × 0.5° bins. We finally add the CARS climatological annual mean to the yearly anomalies to obtain the annual mean time series of Fig. 2. Standard errors are obtained from the standard deviation across sampled bins within each year (July to June), scaled by the square root of their number. Note that years with less than 20 sampled bins were discarded, resulting in quasi-continuous coverage from 1956 onwards.

CMIP5 archive. We analysed all CMIP5 models for which 'piControl', 'historical' and 'rcp85' experiments with potential temperature, salinity and sea ice concentration monthly fields were available. Model outputs were downloaded from the Program for Climate Model Diagnosis and Intercomparison data portal[24] at http://pcmdi9.llnl.gov/esgf-web-fe/. A list of all analysed models along with details on their numerical treatment of oceanic convection is given in Supplementary Table 3.

Pre-industrial control runs use fixed boundary conditions, held at the 1860 level. Historical experiments include the full range of natural and anthropogenic forcings, consistent with observations. RCP8.5 corresponds to a high-emissions scenario that includes time-varying greenhouse gas, stratospheric ozone, anthropogenic aerosols, and solar forcings. Under RCP8.5, the radiative forcing relative to pre-industrial conditions rises continuously to reach about 8.5 W m^{-2} in 2100, and increases for another 150 years in the 22–23 century extension before stabilizing at approximately 12 W m^{-2}.

Only one run (r1i1p1) per model and per experiment was considered. Available pre-industrial control simulations had lengths ranging between 240 and 1,000 years. Historical (1860–2005) and RCP8.5 (2006–2100 or 2006–2300) outputs were concatenated to obtain the climate change time series. Nine models had extended RCP8.5 integrations (2006–2300).

CMIP5 model output analysis. From monthly salinity and temperature fields, we determined mixed layer depths as the depth z at which $\sigma_\theta(z) - \sigma_\theta(10\,\text{m}) = 0.03\,\text{kg m}^{-3}$, where σ_θ is the potential density referenced to the surface[29]. This criterion was found to provide a robust diagnostic of modelled mixed layers in the southern polar regions as deep mixed layers were observed to coincide closely with positive sea surface temperature and sea surface salinity anomalies, as well as low sea ice concentration anomalies, signalling the strong vertical flux of heat and salt. Convection area is defined as the total surface area south of 55° S with a September mixed layer depth exceeding 2,000 m. This depth criterion ensures that only deep convection in the open ocean is taken into account. Convection areas are relatively insensitive to the chosen depth threshold because deep convective overturning was generally observed to extend over most of the water column. September was chosen because maximum convection depths and areas are commonly found at the end of austral winter.

Convective years are defined as years during which the convection area is larger than 100,000 km² (about a third of the observed 1970s Weddell Polynya area). The 11 models featuring no significant open ocean convection are those that do not simulate any convection area above this threshold (with the exception of MIROC-ESM, which convects during the last 100 years of its 630-year-long control run as a result of drifting deep Southern Ocean densities, but exhibits no convective activity during the historical period; see Supplementary Table 2).

References

1. Carsey, F. D. Microwave observation of the Weddell Polynya. *Mon. Weath. Rev.* **108**, 2032–2044 (1980).
2. Martinson, D. G., Killworth, P. D. & Gordon, A. L. A convective model for the Weddell Polynya. *J. Phys. Oceanogr.* **11**, 466–488 (1981).
3. Gordon, A. L. Weddell deep water variability. *J. Mar. Res.* **40**, 199–217 (1982).
4. Parkinson, C. L. On the development and cause of the Weddell Polynya in a sea ice simulation. *J. Phys. Oceanogr.* **13**, 501–511 (1983).
5. Killworth, P. D. Deep convection in the world ocean. *Rev. Geophys.* **21**, 1–26 (1983).
6. Martinson, D. G. in *Deep Convection and Deep Water Formation in the Oceans* (eds Chu, P. C. & Gascard, J. C.) 37–52 (Elsevier Oceanography Series, 1991).
7. Holland, D. M. Explaining the Weddell Polynya—a large ocean eddy shed at Maud Rise. *Science* **292**, 1697–1700 (2001).
8. Gordon, A. L., Visbeck, M. & Comiso, J. C. A possible link between the Weddell Polynya and the Southern Annular Mode. *J. Clim.* **20**, 2558–2571 (2007).
9. Hirabara, M., Tsujino, H., Nakano, H. & Yamanaka, G. Formation mechanism of the Weddell Sea Polynya and the impact on the global abyssal ocean. *J. Oceanogr.* **68**, 771–796 (2012).
10. Heuzé, C., Heywood, K. J., Stevens, D. P. & Ridley, J. K. Southern Ocean bottom water characteristics in CMIP5 models. *Geophys. Res. Lett.* **40**, 1409–1414 (2013).
11. Johnson, G. C. Quantifying Antarctic Bottom Water and North Atlantic Deep Water volumes. *J. Geophys. Res.* **113**, C05027 (2008).
12. Purkey, S. G. & Johnson, G. C. Global contraction of Antarctic Bottom Water between the 1980s and 2000s. *J. Clim.* **25**, 5830–5844 (2012).
13. Azaneu, M., Kerr, R., Mata, M. M. & Garcia, C. A. E. Trends in the deep Southern Ocean (1958–2010): implications for Antarctic Bottom Water properties and volume export. *J. Geophys. Res.* **118**, 4213–4227 (2013).
14. Meehl, G. A., Hu, A., Arblaster, J. M., Fasullo, J. T. & Trenberth, K. E. Externally forced and internally generated decadal climate variability associated with the Interdecadal Pacific Oscillation. *J. Clim.* **26**, 7298–7310 (2013).
15. Orsi, A. H., Smethie, W. M. Jr & Bullister, J. L. On the total input of Antarctic waters to the deep ocean: a preliminary estimate from chlorofluorocarbon measurements. *J. Geophys. Res.* **107**, 3122–3135 (2002).
16. Wüst, G. Der Ursprung der Atlantischen Tiefenwasser. *Gesellsch. f. Erdk. Zeits.* 409–509 (1928).
17. Durack, P. J., Wijffels, S. E. & Matear, R. J. Ocean salinities reveal strong global water cycle intensification during 1950 to 2000. *Science* **336**, 455–458 (2012).
18. Fyfe, J. C., Gillett, N. P. & Marshall, G. J. Human influence on extratropical Southern Hemisphere summer precipitation. *Geophys. Res. Lett.* **39**, L23711 (2012).
19. Rignot, E., Jacobs, S., Mouginot, J. & Scheuchl, B. Ice-shelf melting around Antarctica. *Science* **341**, 266–270 (2013).
20. Gordon, A. L. & Huber, B. A. Southern Ocean winter mixed layer. *J. Geophys. Res.* **95**, 11655–11672 (1990).
21. Galbraith, E. D. *et al.* Climate variability and radiocarbon in the CM2Mc Earth System Model. *J. Clim.* **24**, 4230–4254 (2011).
22. Akitomo, K. Open-ocean deep convection due to thermobaricity: 1. Scaling argument. *J. Geophys. Res.* **104**, 5225–5234 (1999).
23. Martin, T., Park, W. & Latif, M. Multi-centennial variability controlled by Southern Ocean convection in the Kiel Climate Model. *Clim. Dynam.* **40**, 2005–2022 (2013).
24. Taylor, K. E., Stouffer, R. J. & Meehl, G. A. An overview of CMIP5 and the experiment design. *Bull. Am. Meteorol. Soc.* **93**, 485–498 (2012).
25. Latif, M., Martin, T. & Park, W. Southern Ocean sector centennial climate variability and recent decadal trends. *J. Clim.* **26**, 7767–7782 (2013).
26. Church, J. A. *et al.* Revisiting the Earth's sea-level and energy budgets from 1961 to 2008. *Geophys. Res. Lett.* **38**, L18601 (2011).
27. Burke, A. & Robinson, L. F. The Southern Ocean's role in carbon exchange during the last deglaciation. *Science* **335**, 557–561 (2012).
28. Ridgway, K. R., Dunn, J. R. & Wilkin, J. L. Ocean interpolation by four-dimensional weighted least squares—application to the waters around Australasia. *J. Atmos. Oceanic Technol.* **19**, 1357–1375 (2002).
29. de Boyer Montégut, C., Madec, G., Fischer, A. S., Lazar, A. & Iudicone, D. Mixed layer depth over the global ocean: An examination of profile data and a profile-based climatology. *J. Geophys. Res.* **109**, C12003 (2004).
30. Parkinson, C. L., Comiso, J. C. & Zwally, H. J. Nimbus-5 ESMR polar gridded sea ice concentrations. September 1974–1976 Boulder, Colorado USA: National Snow and Ice Data Center. (1999, updated 2004).

Author contributions

All authors shared responsibility for writing the manuscript. C.d.L. assembled and analysed observational data and model output. J.B.P. and E.D.G. conceived and supervised the study. I.M., R.B., E.D.G. and J.B.P. designed the CM2Mc experiments. R.B. performed the CM2Mc experiments.

Additional information

Supplementary information is available in the online version of the paper. Reprints and permissions information is available online at www.nature.com/reprints. Correspondence and requests for materials should be addressed to C.d.L.

Competing financial interests

The authors declare no competing financial interests.